

Analysis of late Quaternary linear dune development in the Thar Desert, India.

Aayush Srivastava^{a*}, Julie A. Durcan^a and David S.G. Thomas^{a, b}

^a School of Geography and the Environment, University of Oxford, Oxford, OX1 3QY,
United Kingdom

^b School of Geography, Archaeology and Environmental Studies, University of the
Witwatersrand, Johannesburg 2050, South Africa

*Corresponding author. E-mail address: aayush.srivastava@ouce.ox.ac.uk (A. Srivastava).

Abstract

Linear dunes are the most widespread dune type worldwide and act as important geoproxies of late Quaternary environmental change in deserts. They are less common in the Thar Desert, India than other dune types, especially parabolic forms, and to date their development history is poorly understood. Here we investigate a linear dunefield in the northern Thar through analysis of a series of excavated full dune profile sites and the application of optically stimulated luminescence (OSL) dating to provide chronometric control. Results show that linear dunes have been present since at least ~58 ka and were active throughout much of the Holocene. The early Holocene, a period marked by strong Indian summer monsoon winds (e.g., Gill et al., 2017), has been shown as the last major phase of dune accumulation recorded in all sites, with ages ranging from ~11.6-8.6 ka. Two spatially restricted records of dune accumulation have also been identified during the later part of Holocene: ~4-3 ka and ~2-1 ka, attributed to localised reworking within the dunes. The suite of luminescence ages generated from the study region confirms the principle recognised in other dunefields (e.g., the southwest Kalahari; Stone and Thomas, 2008) and theoretically (Bailey and

Thomas, 2014) that age records from individual dunes are unlikely to capture the developmental history of dunefields.

Keywords: *Thar Desert, optically stimulated luminescence (OSL) dating, linear dunes, the Holocene, geomorphological change.*

1. Introduction

A range of dune forms are present in the Thar Desert including parabolic, linear, transverse, star and network (e.g., Wasson *et al.*, 1983; Kar, 1993; Moharana *et al.*, 2013; Fig. 1A). The organisation and orientation of these dunes reflects the role of dominant south-west monsoon winds, which have governed aeolian dynamics regionally during the late Quaternary. The presence of superimposed forms, for example young meso-scale dunes on older, bigger parabolic dunes (Srivastava *et al.*, 2019) attests to a more complex history of dune dynamics in the Thar.

Linear dunes, which are the most common desert dune type worldwide, including palaeo-dunes in semi-arid and arid landscapes (Lancaster, 1982; Tsoar, 1989) are relatively uncommon in the Thar. These dunes cover an area of approximately 11,200 km², representing around 7.5 % of all aeolian landforms in the Thar, where parabolic dunes are the most commonly observed dune type (Wasson *et al.*, 1983; Kar, 1993; Moharana *et al.*, 2013). Thar linear dunes occur mostly in the border zone between India and Pakistan in Jaisalmer district in the western part of the desert (Kar, 1987). Other studies have mapped smaller areas of linear dunes in the northern Thar near Bikaner (Saxena and Singh, 1976; Kumar *et al.*, 1993) and the central Thar near Jodhpur (Verstappen, 1968; Kar, 1993) (Fig. 1A). Many of these smaller dunefields,

however, have since been flattened to make way for the expansion of irrigated agriculture, removing landforms and prohibiting their analysis.

Linear dunes in the Thar have often been considered as an 'old system' (e.g., Pandey *et al.*, 1964; Kar, 1993; Singhvi and Kar, 2004; Kar, 2014) with natural vegetation forming an integral part of the dune bodies. The length of these dunes varies across the Thar from more than 10 km in Jaisalmer to 1-2 km in Bikaner and includes dune forms which vary from Y-junctions to clusters of 5-8 linear dunes joining at acute angles which gradually merge with surrounding parabolic or transverse dunefields (Kar, 1987, 1993, 2014). The Y-junction pattern is similar to that of vegetated linear dunes in the north-western Negev (Tsoar and Moller, 1986; Tsoar *et al.*, 2008) and south-western Kalahari (Thomas and Shaw, 1991; Bullard *et al.*, 1995).

Linear dunes have the potential to offer long-term records of past aeolian episodes because of their accumulatory nature (Thomas 1992; Livingstone and Thomas, 1993; Munyikwa, 2005; Telfer *et al.*, 2010), and thus are considered important geoproxy records (Telfer and Hesse, 2013; Thomas, 2013). The accumulation histories of linear dunes reconstructed using luminescence dating have been frequently and consistently used for palaeoenvironmental reconstructions in dryland environments, notably in southern Africa (e.g., Stokes *et al.*, 1997, O'Connor and Thomas, 1999, Telfer and Thomas, 2007, Stone and Thomas, 2008), Australia (e.g., Lomax *et al.*, 2003, Fitzsimmons *et al.*, 2007), Israel (Roskin *et al.*, 2011a,b) and the Arabian Peninsula (e.g., Glennie and Singhvi, 2002; Atkinson *et al.*, 2013; Leighton *et al.*, 2013). As a result, almost a third of the luminescence ages from drylands listed in the INQUA dune database are from linear dunes (Lancaster *et al.*, 2016). In contrast, there are no ages in the database from linear dunes in the Thar Desert because the majority of chronometric studies to date have focussed on parabolic dunes (Thomas *et al.*, 1999;

72 Kar *et al.*, 2001; Singhvi and Kar, 2004; Dhir *et al.*, 2010; Srivastava *et al.*, 2019). The
73 aim of this work therefore, is to apply a spatially intensive sampling strategy and
74 modern luminescence dating techniques to develop a linear dunefield chronology from
75 the Thar and integrate it into existing knowledge of the geomorphic evolution of the
76 Thar dunes and regional palaeoenvironmental interpretations arising from such
77 results.

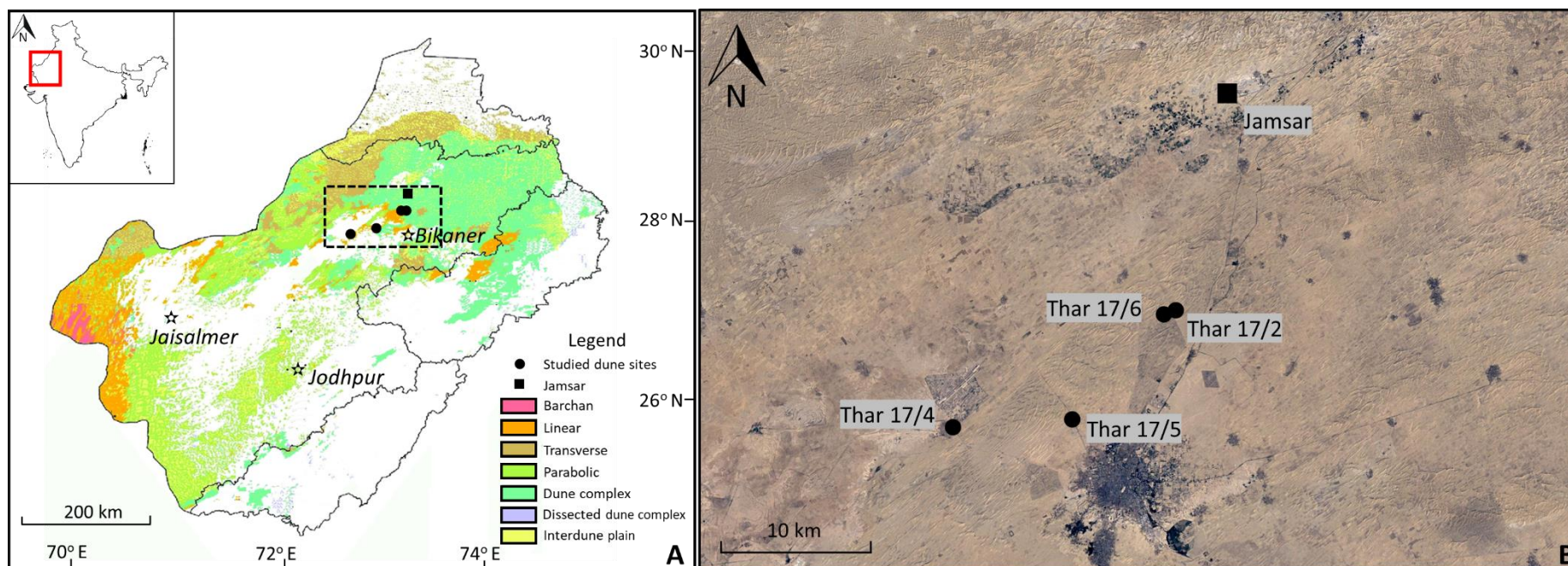


Fig. 1. A. Distribution of different dune types in the Thar Desert, India (after Moharana *et al.*, 2013). B. Sampled linear dune sites (closed circles): Thar 17/2 (28.13728 N, 73.34283 E), Thar 17/4 (28.03315 N, 73.20950 E), Thar 17/5 (28.06017 N, 73.26852 E) and Thar 17/6 (28.13641 N, 73.33286 E).

2. Study sites and methods

2.1. Study sites

The focus of this study is a ~500 km² area of the linear dunefield in the Bikaner area of the northern Thar (Fig. 1B). This area was selected because of its central location, accessibility, and representativeness, based on Google Earth assessment of the linear dunes in the Thar. The Bikaner dunefield today comprises a semiarid to arid landscape with a mean annual precipitation of 200-300 mm and an interannual rainfall coefficient of variation of 47 %. The dunes here are colonised to a varying degree by natural vegetation such as *Lasiurus indicus*, *Capparis decidua*, *Calligonum polygonoides* etc. Dunes range in height from 5 m to 20 m above the interdune areas and are <10 km in crestline length. The orientation of these dunes is in the SW direction controlled by the dominant Indian summer monsoon winds (Fig. 2A).

To identify the timing of periods of linear dune accumulation, field sampling for luminescence dating was conducted at four sites across the dunefield (Fig. 1B): Jaisalmer Bypass (Thar 17/2 and Thar 17/6), Nal (Thar 17/4) and Bajrang Dohra (Thar 17/5) sites. The two Jaisalmer Bypass sites, Thar 17/2 and Thar 17/6, are located <500 m apart near the northern edge of the dunefield. The other two sites, Thar 17/4 and Thar 17/5 fall in the central and south-central part of the dunefield. These were sampled to explore spatial and temporal variability in dune accumulation histories, with the number of sites analysed reflecting accessibility, the logistics of excavating exposures, and the number of samples generated that could effectively be dated while ensuring each sample location was represented by enough samples to capture accumulation histories. The sampled linear dunes are 9-12 m in height relative to the adjacent interdune area and aligned in the dominant direction of monsoon winds. At

107 all four sites, the dune axis was targeted for sampling to obtain dune core sediment
108 presumed to have preserve the maximum thickness of sediments within the dune
109 bodies, and to be least affected by lateral dune movement. Sampled sections were
110 excavated on the crest of these dunes using hydraulic excavators until a hard, calcrete
111 rich layer, suggesting the base of the dune, was reached. The base of the dune was
112 reached at sites Thar 17/2, 17/4 and 17/5, but not at Thar 17/6, where risk of sediment
113 collapse prevented sampling. The dunes were composed of homogenous, usually
114 structureless sand with some fine laminations preserved in the top part of sampled
115 profiles. Sediment faces in the excavated pits were cleaned prior to sampling for
116 optically stimulated luminescence (OSL) dating. All samples were taken at least 0.5 m
117 below the modern dune surfaces and 0.5 m above a hard, calcrete layer, by
118 hammering black light-tight tubes into the cleaned sediment face. Sampling was
119 performed at a 1 m interval unless field examination revealed changes in stratigraphy
120 or sedimentology, in which case additional sampling was carried out to bracket such
121 features.

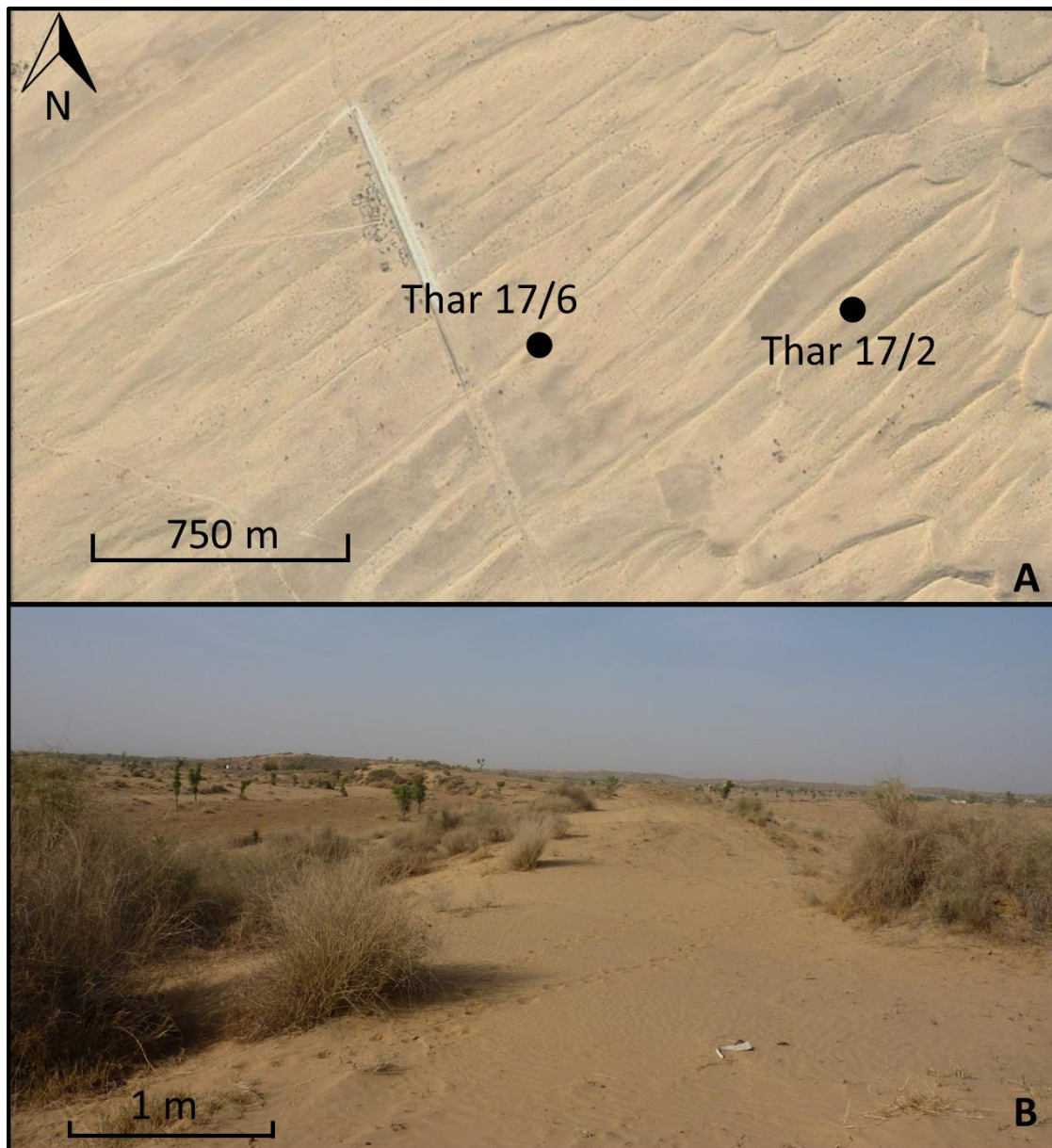


Fig. 2. A. Linear dune pattern in the Bikaner dunefield and location of two studied sites. B. Landscape at site Thar 17/2. The photo is taken from the linear dune crest facing in NE direction.

2.2. Sedimentological analyses

Grain size analyses were conducted using a Malvern Mastersizer Hydro 2000 laser analyser with wet dispersion. Statistics were calculated using Gradistat (Blott and Pye,

2001) following the method of Folk and Ward (1957). Colour analysis was conducted on oven-dried samples using a Munsell colour chart. Organic and carbonate content were determined using sequential loss on ignition at 550 °C and 950 °C (Heiri *et al.*, 2001) and expressed as a percentage of the sample weight.

2.3. Sediment preparation for luminescence dating

Samples were opened and prepared in subdued orange light conditions in the Oxford Luminescence Dating Laboratory. Prior to preparation of sediment for OSL dating, light-exposed sediments from the sample tube ends were removed and reserved for dose rate and sedimentological measurements. Sediments for luminescence dating were treated with hydrochloric acid and hydrogen peroxide to remove carbonate and organic matter, and sieved to isolate the 180-210 µm grain size fraction. Quartz mineral grains were removed from the bulk sample using sodium polytungstate density separation, which was followed by chemical etching using hydrofluoric acid to remove the alpha-irradiated outer surface of the quartz grains and fluorosilicic acid to remove persistent feldspar contamination. After chemical etching, hydrochloric acid was used to remove any fluoride precipitate, prior to re-sieving. Fully prepared dry sediment was mounted onto aluminium discs as a 2 mm (small aliquot) monolayer consisting of ~70 grains (Heer *et al.*, 2012) using Silkospray silicon oil.

2.4. Equivalent dose determination

Equivalent dose (D_e) measurements were made using Risø DA-15 TL/OSL readers (for full reader specification see Srivastava *et al.*, 2019) and a post-infrared blue single aliquot regenerative (SAR) dose protocol (Banerjee *et al.*, 2001). Following pre-heat

plateau and dose recovery tests, a pre-heat of 240°C for 10 s and a cut-heat of 160°C for 0 s were selected for use. The protocol comprised an infrared light (870 nm) stimulation at 50°C for 100 s prior to measurement of the blue-light stimulated ultra-violet luminescence signals at 125°C for 40 s. Dose recovery tests on samples Thar 17/2/4, 17/4/8, 17/5/1, 17/6/2, and 17/6/6, provided ratios of 0.94 ± 0.04 , 0.95 ± 0.04 , 1.00 ± 0.06 , 1.00 ± 0.07 , and 0.96 ± 0.05 , respectively, indicating the suitability of the applied protocol. To ascertain the average number of luminescing signals, single grain analyses of samples on samples Thar 17/2/4, Thar 17/4/2, Thar 17/4/8, Thar 17/5/6, Thar 17/6/6 and Thar 17/6/9 was undertaken, and showed that between 2.4 and 5.0 % of the measured 500 grains gave a discernible luminescence signal after a 50 Gy dose.

Luminescence signals were included in final D_e calculation when the following rejection criteria were satisfied: 1) recuperation less than 5 % (where sample D_e was greater than 1.5 Gy) or 0.25 Gy (for D_e s less than 1.5 Gy); 2) recycling ratio within 10 % of unity, including uncertainties (Murray and Wintle, 2003); and 3) test dose signals 3σ greater than the background. Final D_e determinations for each sample were based upon at least 20 accepted aliquots and were calculated in the R Luminescence package (Kreutzer *et al.*, 2017) using the central age model (CAM) (Galbraith *et al.*, 1999).

2.5. Dose rate determination

Radionuclide concentrations (^{232}Th , ^{238}U and ^{40}K) were measured using inductively coupled plasma mass spectrometry at the Scottish University Environmental Research Centre, East Kilbride. Infinite-matrix dose rates were calculated using the

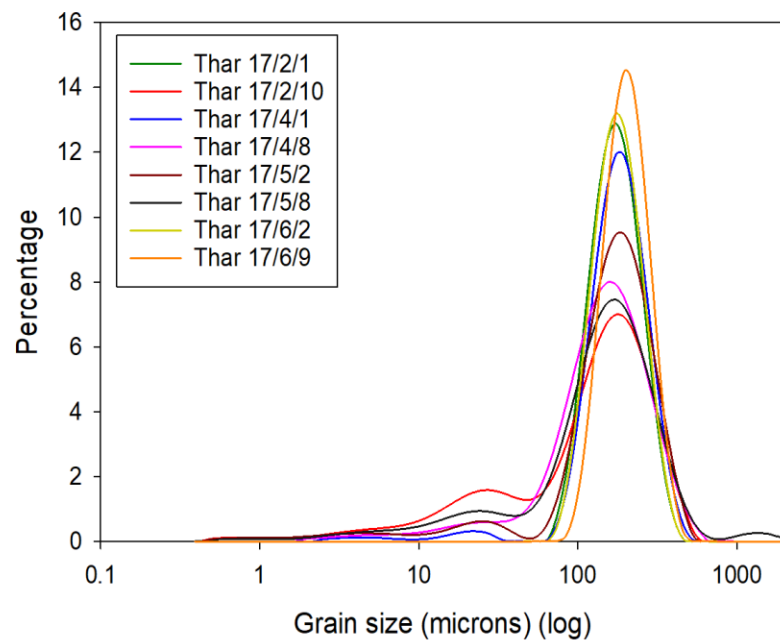
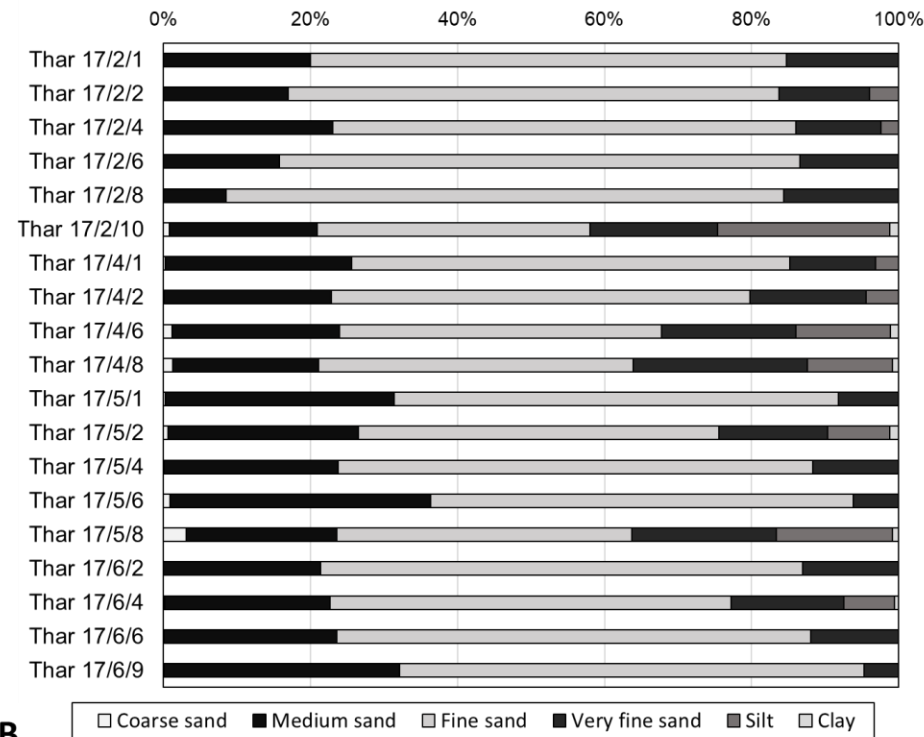
conversion factors of Guerin *et al.* (2011) and were adjusted for attenuation by grain size and chemical etching using the datasets of Guerin *et al.* (2012) and Bell (1979) respectively, as well as a moisture content of 5 ± 2 %. Following Prescott and Hutton (1994), cosmic dose rates were determined from sample longitude, latitude, altitude, and depth. All dose rate calculations were made using the DRAC (v1.2) software of Durcan *et al.* (2015).

3. Results

3.1. Sedimentology

Sedimentological data are provided in Table 1. The samples are consistent in colour within each dune. The majority of samples are unimodal (Fig. 3A), predominantly composed of medium to fine sand, with silt and clay components varying between 0 - 23.5 % and 0 - 1.2 % respectively (Fig. 3B). Mean grain sizes are within the range of ~ 105 – 220 μm , comparable with linear dune sediments, for example in north-eastern Rub' al Khali in Arabia (Leighton *et al.*, 2013) and the north-western Negev (Roskin *et al.*, 2011a). Most samples are well to moderately well sorted with symmetrical and mesokurtic distributions (Table 1). The organic content by weight is less than 2 %, while carbonate content by weight increases with depth in a section, varying between ~ 1 and ~ 5 %. These organic and carbonate values are consistent with other recently reported values from Thar parabolic dune sands (Srivastava *et al.*, 2019).

201

**A****B**

202

Fig. 3. A. Grain size distribution by volume for selected samples from each sampled dune. B. The percentage distribution of different grain sizes for all the samples. Clay <2 μm ; silt = 2-63 μm ; very fine sand = 63-125 μm ; fine sand= 125-250 μm , medium sand = 250-500 μm ; and coarse sand = 500-1000 μm (Blott and Pye, 2001 and references therein).

206

207

Table 1. Sedimentology of samples showing Munsell colour, grain size statistics (in microns), organic and carbonate content.

Sample	Munsell	Mean	Coarse sand (500-1000 µm) (%)	Medium sand (250-500 µm) (%)	Fine sand (125-250 µm) (%)	Very fine sand (63-125 µm) (%)	Silt (2-63 µm) (%)	Clay (<2 µm) (%)	Sorting*	Skewness**	Kurtosis***	Organic content (%)	Carbonate content (%)
Thar 17/2/1	10 YR 5/4	183.0	0.0	20.0	64.7	15.3	0.0	0.0	1.439 (MWS)	-0.001 (S)	0.952 (M)	0.62	1.80
Thar 17/2/2	10 YR 5/4	178.5	0.0	17.0	66.7	12.3	4.0	0.0	1.447 (MWS)	-0.086 (S)	1.072 (M)	0.76	2.31
Thar 17/2/4	10 YR 5/4	188.8	0.0	23.0	63.0	11.6	2.4	0.0	1.459 (MWS)	-0.037 (S)	0.994 (M)	0.87	2.80
Thar 17/2/6	10 YR 5/4	179.9	0.0	15.8	70.8	13.4	0.0	0.0	1.382 (WS)	0.000 (S)	0.956 (M)	0.72	2.10
Thar 17/2/8	10 YR 5/4	168.3	0.0	8.5	75.9	15.6	0.0	0.0	1.336 (WS)	0.001 (S)	0.965 (M)	0.60	3.88
Thar 17/2/10	10YR 5/4	106.8	0.8	20.1	37.1	17.4	23.4	1.2	3.114 (PS)	-0.470 (VFS)	1.226 (L)	1.36	3.94
Thar 17/4/1	10 YR 6/4	191.1	0.3	25.3	59.6	11.7	3.1	0.0	1.500 (MWS)	-0.051 (S)	1.013 (M)	0.58	1.70
Thar 17/4/2	10 YR 6/4	180.2	0.1	22.8	56.9	15.8	4.4	0.0	1.569 (MWS)	-0.088 (S)	1.063 (M)	0.87	2.24
Thar 17/4/6	10 YR 6/4	154.3	1.2	22.8	43.8	18.2	12.9	1.1	2.399 (PS)	-0.356 (VFS)	1.747 (VL)	0.71	2.60
Thar 17/4/8	10 YR 6/4	149.0	1.3	19.8	42.8	23.7	11.6	0.8	2.192 (PS)	-0.258 (FS)	1.463 (L)	0.98	5.06
Thar 17/5/1	10 YR 6/4	208.3	0.3	31.1	60.4	8.2	0.0	0.0	1.441 (MWS)	-0.006 (S)	0.952 (M)	0.88	1.90
Thar 17/5/2	10 YR 6/4	176.6	0.6	25.9	49.1	14.8	8.5	1.2	2.134 (PS)	-0.322 (VFS)	1.877 (VL)	0.87	1.96
Thar 17/5/4	10 YR 6/4	192.4	0.1	23.7	64.5	11.7	0.0	0.0	1.429 (MWS)	0.006 (S)	0.952 (M)	0.51	2.10
Thar 17/5/6	10 YR 6/4	219.0	0.9	35.5	57.4	6.2	0.0	0.0	1.446 (MWS)	0.009 (S)	0.952 (M)	0.48	2.48
Thar 17/5/8	10 YR 6/4	140.4	3.1	20.5	40.1	19.9	15.8	0.8	2.584 (PS)	-0.343 (VFS)	1.567 (VL)	1.65	3.85
Thar 17/6/2	10 YR 5/4	187.5	0.0	21.4	65.5	13.1	0.0	0.0	1.425 (MWS)	0.002 (S)	0.946 (M)	0.60	1.09
Thar 17/6/4	10 YR 5/4	175.7	0.2	22.5	54.5	15.3	6.9	0.6	1.932 (MS)	-0.295 (FS)	1.838 (VL)	0.59	2.20
Thar 17/6/6	10 YR 5/4	191.7	0.1	23.5	64.4	12.0	0.0	0.0	1.431 (MWS)	0.007 (S)	0.951 (M)	0.56	3.21
Thar 17/6/9	10 YR 5/4	214.6	0.1	32.0	63.2	4.7	0.0	0.0	1.381 (WS)	-0.003 (S)	0.956 (M)	0.52	2.78

* MWS= moderately well sorted, WS= well sorted, MS= moderately sorted, PS= poorly sorted.

210 ** FS= finely skewed, VFS= very finely skewed, S= symmetrical.

211 *** L= leptokurtic, VL= very leptokurtic, M= mesokurtic

3.2. Luminescence dating

In general, measured luminescence signals from small aliquots are bright enough to be discernible from the background (Fig. 4A) and are dominated by the quartz fast component in the initial part of the OSL signal (fast ratio > 20; Durcan and Duller, 2011). Single grain analyses confirm the low levels of luminescence sensitivity to dose (2-3 luminescing grains per disc), which ensures that any heterogeneity in D_e distributions should be identified. The heterogeneity or over-dispersion (σ_d), in D_e distributions for the majority samples in this study ranges between 20 % and 45 % (Table 2), with slightly higher values (~45%) observed for two of the younger samples. These σ_d values are in line with values calculated from other single aliquots of dune samples in the central Thar (σ_d = 20-40 %; Srivastava *et al.*, 2019), single grains of dune samples from the northern Thar margin (σ_d = 30-50 %; Durcan *et al.*, 2019) and are comparable to linear dunes studies elsewhere (e.g., the Negev, σ_d = 10-60 %; Roskin *et al.*, 2011a). Overdispersion can be caused by a combination of intrinsic factors, such as natural variability of quartz (Thomsen *et al.*, 2012 and references therein), as well as extrinsic sources, such as heterogeneous bleaching (e.g., Olley *et al.*, 2004), post-depositional mixing of sediments (e.g., Bateman *et al.*, 2003; 2007; Kristensen, 2015), and dosimetric variability (e.g., Nathan *et al.*, 2003; Mayya *et al.*, 2006); and instrumental sources which have a small contribution (e.g., Thomsen *et al.*, 2005; Cunningham *et al.*, 2011). As discussed, the observed σ_d values for this suite of data is relatively low, and in line with other published values from aeolian, dryland contexts. σ_d values from dose recovery tests were <5 %, and therefore we hypothesise external factors as the source of the observed variability. σ_d due to incomplete bleaching is unlikely, given the deposition by aeolian processes (Duller, 2004; Singhvi and Porat, 2008), and samples were carefully collected from visibly

undisturbed strata, which should minimise D_e variability as a result of post-depositional mixing. We, therefore, hypothesise mild microdosimetric variability as a source of variability in D_e distributions. It has been demonstrated empirically and through modelling that microdosimetric variability may contribute significantly to variations in D_e s for well-bleached samples (up to ~45- 50 %; see Mayya *et al.*, 2006; Cunningham *et al.*, 2012; Guérin *et al.*, 2015; Jankowski and Jacobs, 2018). In this context of relatively low σ_d values, which are in line with other published studies, and given that the D_e distributions tend to be symmetrical around a central value (e.g., Fig. 4B), the CAM (Galbraith *et al.*, 1999) has been used for final D_e calculation. This follows the rationale of other dryland-based studies, such as Parton *et al.* (2015) and Durcan *et al.* (2019).

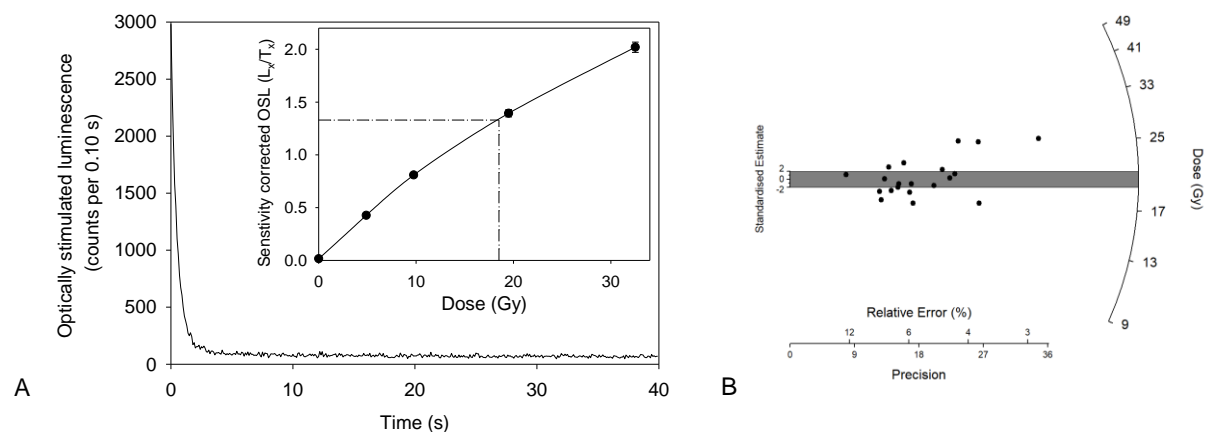


Fig. 4. A. An example OSL signal from sample Thar 17/2/6, and the dose response curve from the same aliquot (inset) B. Radial plot of individual D_e s for Thar 17/2/6 ($\sigma_d = 23\%$).

255

256 3.2.1. Calculation of minimum ages

257 One of the factors which limits the upper dateable range of OSL dating is signal
258 saturation. A quartz OSL signal can be considered saturated if either the natural signal
259 does not intercept the dose response curve (DRC) or if the natural signal interpolates
260 onto the flat, asymptotic part of the DRC (e.g., Fig. 5). Interpolation of the natural signal
261 from the asymptote of the saturated DRC results in a large and asymmetric uncertainty
262 in D_e (Murray *et al.*, 2002; Murray and Funder, 2003) and therefore should be avoided
263 where possible. Wintle and Murray (2006) suggest that a prudent upper dating limit for
264 saturated signals is the $2D_0$ parameter, which represents ~85% of the upper saturation
265 point obtained from the DRC. D_0 is derived from the fitting of the DRC with a single
266 saturating exponential function, $I = I_0 (1 - \exp^{-D/D_0})$ where I is the OSL intensity after a
267 dose (D), I_0 is the saturation intensity and D_0 is the dose level characteristic of the
268 DRC (Wintle and Murray, 2006).

269 In this study, a signal was considered saturated if there was no interpolation on the
270 DRC or if the calculated D_e was greater than $2D_0$. A sample was considered saturated
271 when more than 50 % of measured accepted aliquots were saturated, and a minimum
272 age was calculated using the mean $2D_0$ values of all accepted aliquots. These
273 minimum ages are reported to the nearest integer and without an uncertainty,
274 reflecting that the 'true' D_e is in excess of quoted minimum. Two samples are
275 considered saturated (Table 2): Thar 17/2/10 (15/27 aliquots saturated) and Thar
276 17/5/8 (14/24) and yielded minimum ages of >58 ka and >48 ka respectively.

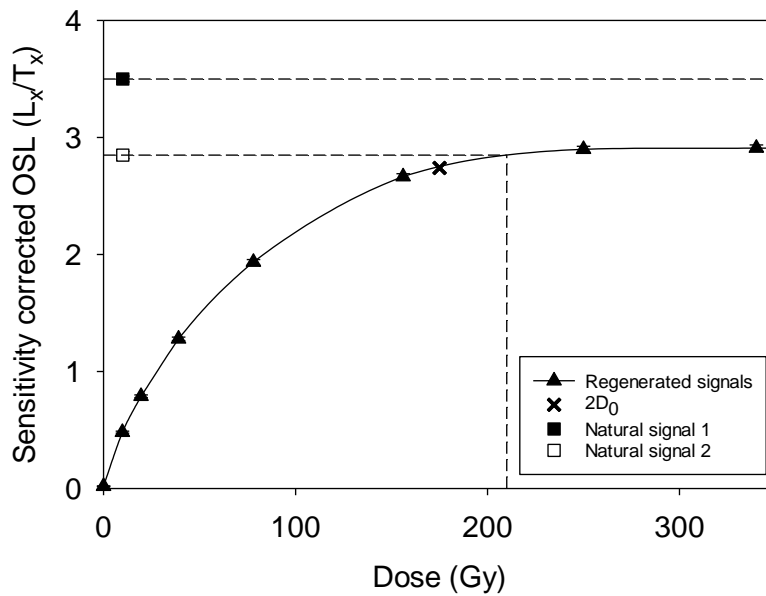


Fig. 5. The two types of OSL signal considered saturated in this study. i) where natural signal does not intercept the dose response curve (natural signal 1 square symbol) and ii) when the interpolated D_e exceeds $2D_0$ (natural signal 2 open square symbol).

3.2.2. Luminescence ages

A summary of the luminescence dating results is provided in Table 2 along with stratigraphic sections (Fig. 6A) and age-depth profiles (Fig. 6B). At all four sites, OSL ages (including uncertainties) are in stratigraphic order and 17 of the 19 samples date to the Holocene, 10 of which date to the early part of the Holocene. Site Thar 17/2 depicts a Pleistocene feature with the oldest age at 9 m depth having a minimum age of >58 ka. At 7 and 3 m depths, sample ages are within uncertainties: 8.81 ± 0.71 ka (Thar 17/2/8) and 8.62 ± 0.64 ka (Thar 17/2/4) old respectively. Sample Thar 17/2/1 shows that the uppermost 0.8 m of dune sediments accumulated in the last ~ 500 years (Thar 17/2/1) and is immediately underlain by a 4.07 ± 0.44 ka old sample at 0.9 m

(Thar 17/2/2). The five samples from Thar 17/5 dune show a similar dune accumulation pattern to Thar 17/2 where the basal dune unit is atleast ~48 ka old (Thar 17/5/8) and is overlain by 2 m dune which accumulated between 9.38 ± 0.82 ka (Thar 17/5/6) and 9.27 ± 0.64 ka (Thar 17/5/4). The top 1.6 m of sediments at Thar 17/5 recorded dune activity in the last ~150 years (Thar 17/5/1). The site 17/4 preserves only Holocene accumulation with the oldest sample at 11 m dating to 11.61 ± 0.82 ka (Thar 17/4/8). 7 m of dune sand accumulation occurred between 10.52 ± 0.99 ka (Thar 17/4/6) and 8.79 ± 0.67 ka (Thar 17/4/2). The uppermost sample, taken 0.5 m below the dune surface, dates to 3.01 ± 0.24 ka (Thar 17/4/1). At site Thar 17/6, between 9.5 and 6 m down section, sample ages are within uncertainties- 9.39 ± 0.69 ka (Thar 17/6/9) and 9.38 ± 0.71 ka (Thar 17/6/6) old. The top 2 m dune is recent, dating from 0.34 ± 0.03 ka (Thar 17/6/2).

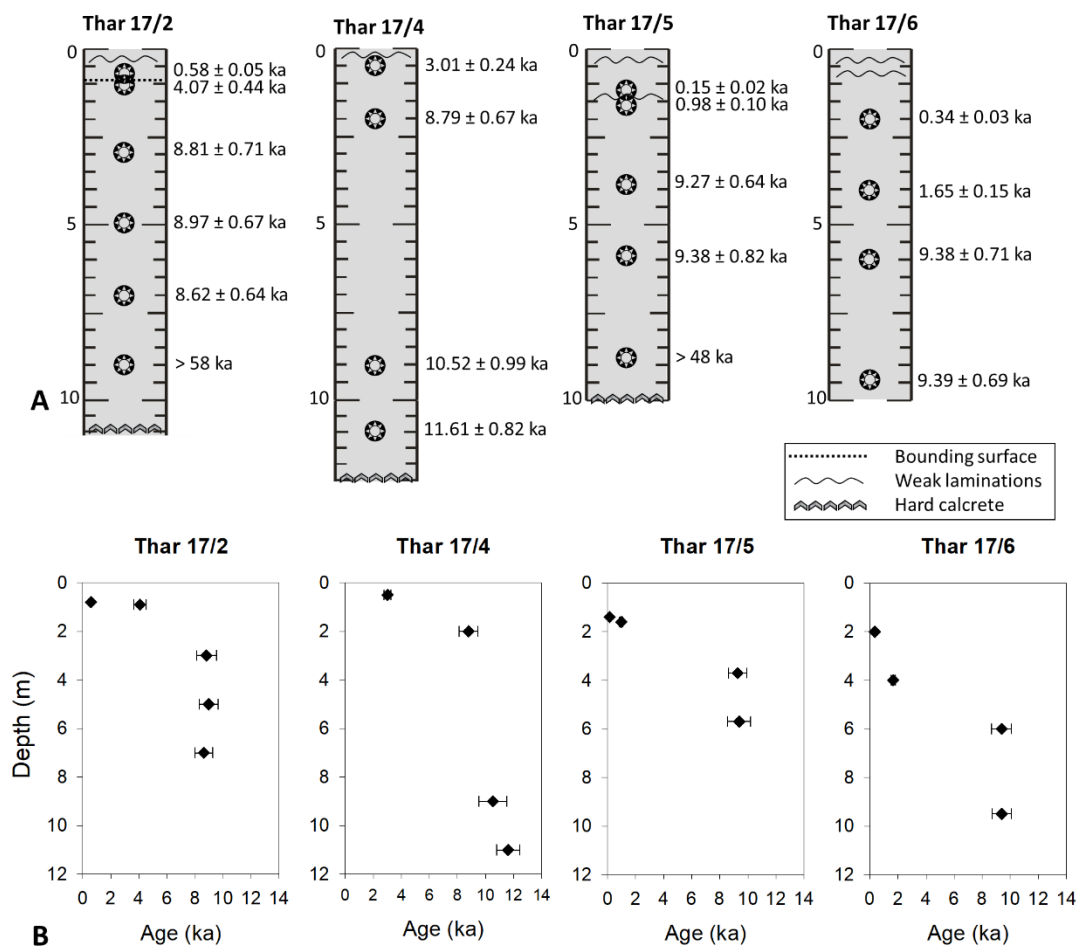


Fig. 6. A. Stratigraphic sections and OSL ages for the sampled sites investigated in this study. Sample depth are in metres. Note the sections comprised largely homogenous and structureless sand with very few laminations or other sedimentological features. B. Age-depth profiles for all four sites. The minimum ages for samples Thar 17/2/10 (>58 ka) and 17/5/8 (>48 ka) are not displayed.

312 **Table 2. Summary OSL data. Equivalent doses (D_e), dose rates (\dot{D}), and ages are shown to two decimal places, with all calculations made prior to rounding.**
313 **Minimum D_e s and ages are calculated for samples Thar 17/2/10 and Thar 17/5/8 due to signal saturation and are quoted to the nearest integer, without**
314 **uncertainties. All ages are relative to the year 2018.**

Sample	Depth (m)	Discs accepted (measured)	Over-dispersion (%)	D_e (Gy)	Beta \dot{D} (Gy.ka ⁻¹)	Gamma \dot{D} (Gy.ka ⁻¹)	Cosmic \dot{D} (Gy.ka ⁻¹)	Envir \dot{D} (Gy.ka ⁻¹)	Age (ka)
Thar 17/2/1	0.8	26 (38)	34.3 ± 4.8	1.22 ± 0.08	1.24 ± 0.11	0.68 ± 0.05	0.19 ± 0.02	2.10 ± 0.12	0.58 ± 0.05
Thar 17/2/2	0.9	22 (36)	36.6 ± 6.1	8.36 ± 0.78	1.17 ± 0.10	0.71 ± 0.05	0.18 ± 0.02	2.06 ± 0.11	4.07 ± 0.44
Thar 17/2/4	3.0	25 (46)	28.0 ± 4.0	19.74 ± 1.18	1.25 ± 0.11	0.85 ± 0.05	0.14 ± 0.01	2.24 ± 0.12	8.81 ± 0.71
Thar 17/2/6	5.0	21 (43)	22.3 ± 3.7	19.82 ± 1.04	1.24 ± 0.10	0.86 ± 0.06	0.11 ± 0.01	2.21 ± 0.12	8.97 ± 0.67
Thar 17/2/8	7.0	21 (27)	24.3 ± 3.8	19.64 ± 1.05	1.25 ± 0.10	0.94 ± 0.06	0.09 ± 0.01	2.28 ± 0.12	8.62 ± 0.64
Thar 17/2/10	9.0	27 (30)	-	>125	1.26 ± 0.11	0.82 ± 0.05	0.08 ± 0.01	2.15 ± 0.12	> 58
Thar 17/4/1	0.5	21 (32)	28.4 ± 4.4	8.24 ± 0.51	1.44 ± 0.11	1.10 ± 0.07	0.21 ± 0.02	2.74 ± 0.14	3.01 ± 0.24
Thar 17/4/2	2.0	24 (35)	27.0 ± 3.9	20.39 ± 1.13	1.27 ± 0.10	0.89 ± 0.06	0.16 ± 0.02	2.32 ± 0.12	8.79 ± 0.67
Thar 17/4/6	9.0	24 (48)	37.0 ± 5.5	24.97 ± 1.94	1.35 ± 0.11	0.95 ± 0.06	0.08 ± 0.01	2.37 ± 0.13	10.52 ± 0.99
Thar 17/4/8	11.0	30 (43)	24.8 ± 3.3	25.23 ± 1.15	1.26 ± 0.10	0.85 ± 0.06	0.06 ± 0.01	2.17 ± 0.12	11.61 ± 0.82
Thar 17/5/1	1.4	22 (28)	44.3 ± 8.0	0.32 ± 0.03	1.28 ± 0.11	0.72 ± 0.05	0.17 ± 0.02	2.17 ± 0.13	0.15 ± 0.02
Thar 17/5/2	1.6	20 (36)	42.8 ± 6.8	2.51 ± 0.24	1.36 ± 0.11	1.04 ± 0.07	0.17 ± 0.02	2.56 ± 0.13	0.98 ± 0.10
Thar 17/5/4	3.7	23 (46)	19.2 ± 2.9	19.53 ± 0.79	1.23 ± 0.11	0.74 ± 0.05	0.13 ± 0.01	2.11 ± 0.12	9.27 ± 0.64
Thar 17/5/6	5.7	20 (46)	27.9 ± 4.8	18.75 ± 1.23	1.21 ± 0.11	0.68 ± 0.05	0.11 ± 0.01	2.00 ± 0.12	9.38 ± 0.82
Thar 17/5/8	8.7	24 (33)	-	>127	1.44 ± 0.11	1.13 ± 0.08	0.08 ± 0.01	2.65 ± 0.13	> 48
Thar 17/6/2	2.0	22 (34)	33.0 ± 5.3	0.84 ± 0.06	1.34 ± 0.11	0.95 ± 0.06	0.16 ± 0.02	2.44 ± 0.13	0.34 ± 0.03
Thar 17/6/4	4.0	20 (35)	29.4 ± 5.0	3.72 ± 0.26	1.30 ± 0.11	0.83 ± 0.06	0.13 ± 0.01	2.26 ± 0.12	1.65 ± 0.15
Thar 17/6/6	6.0	24 (34)	30.4 ± 4.5	20.08 ± 1.07	1.22 ± 0.10	0.82 ± 0.05	0.10 ± 0.01	2.14 ± 0.12	9.38 ± 0.71
Thar 17/6/9	9.5	20 (46)	21.6 ± 3.9	22.10 ± 1.15	1.33 ± 0.11	0.96 ± 0.06	0.07 ± 0.01	2.35 ± 0.12	9.39 ± 0.69

315

316

4. Discussion

Previous chronometric investigations of dunes in the northern Thar Desert have been limited and have focussed chiefly on transverse and parabolic dunes (Kar *et al.*, 1998; Thomas *et al.*, 1999). These studies often relied on sampling pre-existing exposures and used older and now mostly redundant multiple aliquot luminescence dating techniques (Duller, 2004). The ages from these studies provided evidence of mid to late- Holocene dune activity (Kar *et al.*, 1998; Thomas *et al.*, 1999; Singhvi and Kar, 2004). The oldest ages in our new suite of data are from full depth profiles of sites Thar 17/5 and Thar 17/2. Though these two ages of > 48 ka (Thar 17/5/8) and > 58 ka (Thar 17/2/10) are minimum age estimates, they are still considerably older than the records in previously published chronologies (Thomas *et al.*, 1999; Singhvi and Kar, 2004), and provide the first reported occurrence of pre-Holocene dune activity in the northern Thar. This is important considering previous studies from southern, central and eastern Thar have presented dune records dating to >50 ka and attested to the antiquity of the desert (Chougankar *et al.*, 1999; Dhir *et al.*, 2010; Singhvi *et al.*, 2010) while records from the northern Thar dunes were limited to the Holocene.

A significant component of our new dataset is evidence of early Holocene dune accumulation, and importantly this is recorded at all four sites, spanning 11.61 ± 0.82 ka to 8.62 ± 0.64 ka (Fig. 6B). Thick sediment accumulations are recorded during this period: 2 m and 3.5 m of sediment occurred at ~9.4 ka at sites Thar 17/5 and Thar 17/6 respectively. At site Thar 17/2, a 4 m thick dune accumulation dates to slightly later (~8.8 ka), and at Thar 17/4, the lowermost 7 m dune sand accumulated between 11.61 ± 0.82 ka and 8.79 ± 0.67 ka. At this site this translates to an estimated accumulation rate of ~ 2.5 m.ka⁻¹. Regionally, comparable early Holocene net accumulation rates have been reported from NE-SW trending linear dune studies in

the monsoon dominated northeast Rub 'al-Khali Desert (Atkinson *et al.*, 2011, 2012). The early Holocene has been identified as a period marked by strong monsoonal winds compared to the late Holocene, evidenced by the enhanced upwelling off the coast of Oman (Gupta *et al.*, 2003; Fig. 7) and a large wind stress curl across the western Arabian Sea (Gill *et al.*, 2017; Fig. 7). Within the Thar Desert, the parabolic dunefield ~200 km south of the study area (Srivastava *et al.*, 2019) and dunes associated with the Ghaggar-Hakra palaeochannel along the northern desert margin (Durcan *et al.*, 2019) also recorded early Holocene accumulation. The data presented here demonstrate that the last major widespread dune accumulation in the Thar was not limited to the late glacial period (~17 - ~11 ka), but that major aeolian dynamism persisted into the early Holocene until ~8.6 ka.

In our study, only two dates identify mid to late-Holocene dune accumulation (4.07 ± 0.44 ka at Thar 17/2/2 and 3.01 ± 0.24 ka at Thar 17/4/1 (Table 2), both of which were sampled from within 1 m of the dune crest. The mid to late- Holocene dune activity, which resulted in thinner sediment accumulations compared to the early Holocene, suggests that dune activity in the region was less pervasive in terms of dune accumulation during the later part of the Holocene, with thicker units reflecting periods of more intensive dune activity (Telfer *et al.*, 2010;). Two sites (Thar 17/5 and 17/6) record seemingly more localised dune accumulation between 1.65 ± 0.15 - 0.98 ± 0.11 ka, which could be spatially restricted in nature or the result of localised reworking within the dune system. Unlike the early Holocene, the age depth profiles are more variable between the four studied sites during the mid- and late-Holocene (Fig. 6B) suggesting that individual dune profiles do not capture temporally comprehensive accumulation phases even in a spatially intensive dunefield. Telfer *et al.* (2010) and Bailey and Thomas (2014), through their modelling work, have suggested that

preservation potential is unlikely to be equal spatially and temporally within a dune system, due to the interaction of exogenous and endogenous (stochastic) influences on accumulation. Stone and Thomas (2008), in their study of linear dunes in southwest Kalahari, also showed that only some accumulation phases are consistently recorded between dunes and individual dune profiles do not offer a temporal record even for a small region. Here, the younger phases of dune accumulation are preserved in pockets in three studied dunes, while absent in Thar 17/4, where the uppermost sample (0.5 m from the crest) yielded an age of 3.01 ± 0.24 ka. The absence of any common accumulation phases dating to the late Holocene could be due to differential preservation between the dunes or phases being missed in sampling. However, sampling at shallow depth of 0.5 m at Thar 16/4 should have minimised sampling bias towards younger phases. Likewise, at Thar 17/2 there is a jump from 0.58 ± 0.05 ka (Thar 17/2/1) to 4.07 ± 0.44 ka (Thar 17/2/2) over just 0.1 m, where a bounding surface exists, suggests that missing an accumulation phase through sampling is not likely to be the major cause.

Although the INQUA Dunes Atlas chronologic database does not include any dated linear dune sites in the Thar, there are records from at least one dune site from Jamsar in the Bikaner region (Fig. 1B). Thomas *et al.* (1999) described the sampled feature as a linear dune site while later reviews designated it as a parabolic dune (Singhvi and Kar, 2004; Lancaster *et al.*, 2016). Jamsar, which appears to be a linear dune site from Google Earth analysis, was a 3.9 m exposed dune section on the margins of an ephemeral lake studied by Thomas *et al.* (1999) and the authors reported 6 luminescence ages suggesting dune activity between 5.3 ± 0.7 ka and 4.7 ± 0.9 ka, and within the last 2000 years (Fig. 7). These ages were calculated using the multiple aliquot additive dose (MAAD) protocol that was widely used in the early decades of

luminescence dating applications to sediments. It must be noted that earlier protocols did not explicitly check for changes in luminescence sensitivity, therefore potentially adding an element of unreliability to them (Stokes *et al.*, 2000; Duller, 2004). Duller and Augustinus (2006) demonstrated the importance of checking the validity of luminescence dating results obtained using older protocols by dating the same samples from a stabilised linear dune in Tasmania and showed that MAAD protocol methods overestimated D_e values by up to 84 % compared against SAR. Singhvi *et al.* (2010) presented SAR and MAAD ages for four dune samples from the Thar where MAAD ages overestimated the SAR ages by 15-53%. It is therefore possible that previously published ages from Jamsar dune feature (Thomas *et al.*, 1999) are likely maximum ages for sediment accumulation.

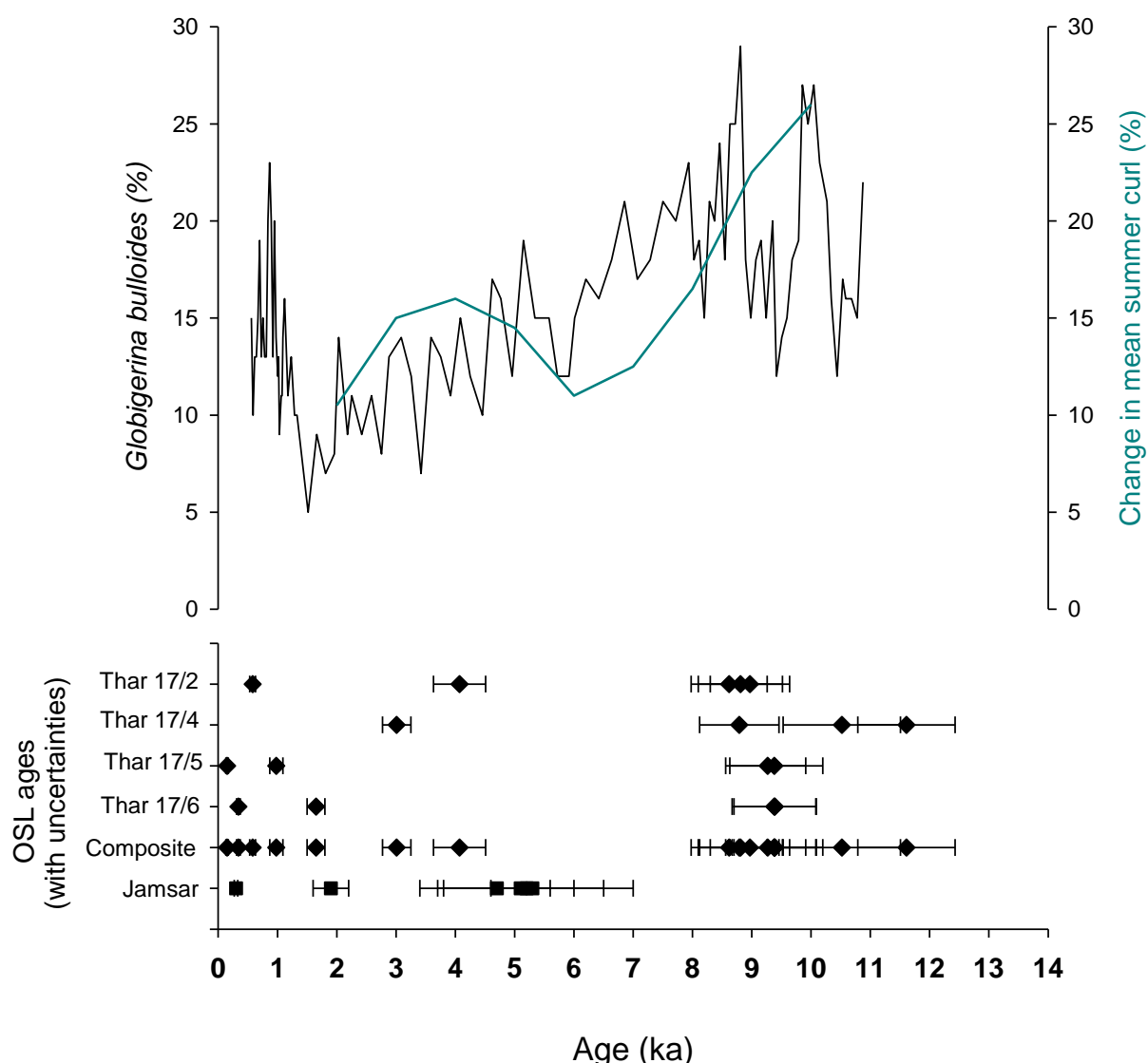


Fig. 7. Thar linear dune OSL ages plotted against reconstructions of *G. bulloides* percentage (Gupta *et al.*, 2003) and percentage change in wind stress curl (blue) (Gill *et al.*, 2017). The diamonds represent the ages determined in this study using post IR blue SAR protocol, while the squares are the MAAD OSL ages calculated by Thomas *et al.* (1999).

The ages from the last millennium have been calculated at the crestal parts of three of the four studied dune sites (Fig. 6A). The site Thar 17/2 recorded 0.8 m of dune accumulation in last ~500 years, Thar 17/5 recorded 1.4 m of accumulation in last

~150 years and Thar 17/6 recorded 2 m of accumulation in the last ~350 years. These thicker units reflect the preservation bias towards younger sediments (Bailey and Thomas, 2014) and the absence of any late Holocene feature at site Thar 17/4 further confirm that individual dune profiles only provide partial information about the past changes. The parabolic dunes in the vicinity of the study area have also witnessed dune accumulation in the last millennium but those are significantly widespread with higher accumulation rates (Srivastava *et al.*, 2019). This difference in dune accumulation rates could be attributed to parabolic dunes being more sensitive to natural and anthropogenic disturbances (e.g., Hugenholtz and Wolfe, 2005; Girardi and Davis, 2010), and the changing landscape in the Thar (Srivastava *et al.*, 2019 and references therein). Nevertheless, the modern ages not only suggest that the Thar linear dunes remained active in later parts of the Holocene but also questions whether these dunes can be grouped under an 'old system' as previously implied (e.g., Pandey *et al.*, 1964; Kar, 1993; Singhvi and Kar, 2004). Similar active and partially-active linear dunes have also been reported from the Negev (Roskin *et al.*, 2011a), the Kalahari (Telfer and Thomas, 2007), the Strzelecki (Lomax *et al.*, 2003) and the Tirari Deserts (Fitzsimmons *et al.*, 2007).

5. Conclusions

This study presents a suite of OSL ages from intensively sampled linear dunes in the Thar Desert, India. The dataset show variability in dune activity between sites in terms of timing and nature of dune accumulation. In general, the record is characterised by consistent and rapid dune accumulation in the early Holocene, and multiple, distinct phases during the mid and late Holocene. The early Holocene period is the most active dune accumulation period which correlates with other Thar dunes records (Srivastava *et al.*, 2019) and wider regional geoproxy evidence. The OSL ages show that the linear

dunes in the Thar have remained active, accumulating sediment during the Holocene. The accumulation of up to 2 m of dune sediment in recent times rules out the earlier notion of classifying linear dunes as belonging to an 'old' Thar Desert system. The suite of ages also presents the first reported records of pre-Holocene dune activity in the northern Thar, albeit as minimum ages, and affirms findings from other desert dunefields that linear dunes preserve a relatively longer chronology. As dune records are increasingly being incorporated to wider palaeoenvironmental studies, our study emphasises on the importance of intensive dunefield sampling, rather than focusing on single dune profiles which do not capture temporally comprehensive accumulation phases, as done in the majority of previous studies in the Thar.

Acknowledgments

The doctoral studies of the first author are funded by the Clarendon Scholarship, University of Oxford. The authors thank the John Fell Fund, University of Oxford (Grant Number 132/062) for providing funding for fieldwork and lab analyses. The first author also thanks the International Society for Aeolian Research for supporting attendance at the 10th International Conference on Aeolian Research in Bordeaux (2018), where this work was initially presented. The authors thank the anonymous reviewers for their comments and suggestions.

References

- Atkinson, O. A., Thomas, D. S. G., Goudie, A. S., Bailey, R. M., 2011. Late Quaternary chronology of major dune ridge development in the northeast Rub'al-Khali, United Arab Emirates. *Quaternary Research* 76, 93-105.
- Atkinson, O. A., Thomas, D. S. G., Goudie, A. S., Parker, A. G., 2012. Holocene development of multiple dune generations in the northeast Rub'al-Khali, United Arab Emirates. *The Holocene* 22, 179-189.

465 Atkinson, O. A., Thomas, D. S. G., Parker, A. G., Goudie, A. S., 2013. Late Quaternary
466 humidity and aridity dynamics in the northeast Rub'al-Khali, United Arab Emirates:
467 implications for early human dispersal and occupation of eastern Arabia. *Quaternary*
468 *International* 300, 292-301.

469 Bailey, R. M., Thomas, D. S. G., 2014. A quantitative approach to understanding dated
470 dune stratigraphies. *Earth Surface Processes and Landforms* 39, 614-631.

471 Banerjee, D., Murray, A. S., Bøtter-Jensen, L., Lang, A., 2001. Equivalent dose
472 estimation using a single aliquot of polymineral fine grains. *Radiation*
473 *Measurements* 33, 73-94.

474 Bateman, M. D., Boulter, C. H., Carr, A. S., Frederick, C. D., Peter, D., Wilder, M.,
475 2007. Detecting post-depositional sediment disturbance in sandy deposits using
476 optical luminescence. *Quaternary Geochronology* 2, 57-64.

477 Bateman, M. D., Frederick, C. D., Jaiswal, M. K., Singhvi, A. K., 2003. Investigations
478 into the potential effects of pedoturbation on luminescence dating. *Quaternary*
479 *Science Reviews* 22, 1169-1176.

480 Bell, W. T., 1979. Attenuation factors for the absorbed radiation dose in quartz
481 inclusions for thermoluminescence dating. *Ancient TL* 8, 12.

482 Blott, S. J., Pye, K., 2001. GRADISTAT: a grain size distribution and statistics package
483 for the analysis of unconsolidated sediments. *Earth surface processes and*
484 *Landforms* 26, 1237-1248.

485 Bullard, J. E., Thomas, D. S. G., Livingstone, I., Wiggs, G. F. S., 1995. Analysis of
486 linear sand dune morphological variability, southwestern Kalahari
487 Desert. *Geomorphology* 11, 189-203.

488 Chougankar, M. P., Raghav, M. S., Rajaguru, S. N., Kar, A., Singhvi, A. K., Nambi,
489 K. S. V., 1999. Luminescence dating results of dune profiles from margins of Thar
490 desert and their implications. *Man Environ* 24, 21-26.

491 Cunningham, A. C., DeVries, D. J., Schaart, D. R., 2012. Experimental and
492 computational simulation of beta-dose heterogeneity in sediment. *Radiation*
493 *Measurements* 47, 1060-1067.

494 Cunningham, A. C., Wallinga, J., Minderhoud, P. S., 2011. Expectations of scatter in
495 equivalent-dose distributions when using multi-grain aliquots for OSL
496 dating. *Geochronometria* 38, 424.

497 Dhir, R. P., Singhvi, A. K., Andrews, J. E., Kar, A., Sareen, B. K., Tandon, S. K.,
498 Kailath, A. Thomas, J. V., 2010. Multiple episodes of aggradation and calcrete
499 formation in Late Quaternary aeolian sands, Central Thar Desert, Rajasthan,
500 India. *Journal of Asian Earth Sciences* 37, 10-16.

501 Duller, G. A. T., 2004. Luminescence dating of Quaternary sediments: recent
502 advances. *Journal of Quaternary Science* 19, 183-192.

503 Duller, G. A. T., Augustinus, P. C., 2006. Reassessment of the record of linear dune
504 activity in Tasmania using optical dating. *Quaternary Science Reviews* 25, 2608-2618.

505 Durcan, J. A., Duller, G. A. T., 2011. The fast ratio: a rapid measure for testing the
506 dominance of the fast component in the initial OSL signal from quartz. *Radiation*
507 *Measurements* 46, 1065-1072.

508 Durcan, J. A., King, G. E., Duller, G. A. T., 2015. DRAC: Dose Rate and Age Calculator
509 for trapped charge dating. *Quaternary Geochronology* 28, 54-61.

510 Durcan, J. A., Thomas, D. S. G., Gupta, S., Pawar, V., Singh, R. N., Petrie, C. A.,
511 2017. Holocene landscape dynamics in the Ghaggar-Hakra palaeochannel region at
512 the northern edge of the Thar Desert, northwest India. *Quaternary International*.

513 Fitzsimmons, K. E., Rhodes, E. J., Magee, J. W., Barrows, T. T., 2007. The timing of
514 linear dune activity in the Strzelecki and Tirari Deserts, Australia. *Quaternary Science*
515 *Reviews* 26, 2598-2616.

516 Folk, R. L., Ward, W. C., 1957. Brazos River bar, Texas- a study in the significance
517 of grain size parameters. *Journal of Sedimentary Research* 27, 3-26.

518 Galbraith, R. F., Roberts, R. G., Laslett, G. M., Yoshida, H., Olley, J. M., 1999. Optical
519 dating of single and multiple grains of quartz from Jinmium rock shelter, northern
520 Australia: Part I, experimental design and statistical models. *Archaeometry* 41, 339-
521 364.

522 Gill, E. C., Rajagopalan, B., Molnar, P. H., Kushnir, Y., Marchitto, T. M., 2017.
523 Reconstruction of Indian summer monsoon winds and precipitation over the past
524 10,000 years using equatorial pacific SST proxy records. *Paleoceanography* 32, 195-
525 216.

526 Girardi, J. D., Davis, D. M., 2010. Parabolic dune reactivation and migration at
527 Napeague, NY, USA: Insights from aerial and GPR imagery. *Geomorphology* 114,
528 530-541.

529 Glennie, K. W., Singhvi, A. K., 2002. Event stratigraphy, paleoenvironment and
530 chronology of SE Arabian deserts. *Quaternary Science Reviews* 21, 853-869.

531 Guérin, G., Jain, M., Thomsen, K. J., Murray, A. S., Mercier, N., 2015. Modelling dose
532 rate to single grains of quartz in well-sorted sand samples: The dispersion arising from
533 the presence of potassium feldspars and implications for single grain OSL
534 dating. *Quaternary Geochronology* 27, 52-65.

535 Guérin, G., Mercier, N., Adamiec, G., 2011. Dose-rate conversion factors: update.
536 *Ancient TL* 29, 5-8.

537 Guérin, G., Mercier, N., Nathan, R., Adamiec, G., Lefrais, Y., 2012. On the use of the
538 infinite matrix assumption and associated concepts: a critical review. *Radiation*
539 *Measurements* 47, 778-785.

540 Gupta, A. K., Anderson, D. M., Overpeck, J. T., 2003. Abrupt changes in the Asian
541 southwest monsoon during the Holocene and their links to the North Atlantic
542 Ocean. *Nature* 421, 354-357.

543 Heer, A. J., Adamiec, G., Moska, P., 2012. How many grains are there on a single
544 aliquot. *Ancient TL* 30, 9-16.

545 Heiri, O., Lotter, A. F., Lemcke, G., 2001. Loss on ignition as a method for estimating
546 organic and carbonate content in sediments: reproducibility and comparability of
547 results. *Journal of paleolimnology* 25, 101-110.

548 Hugenholtz, C. H., Wolfe, S. A., 2005. Recent stabilization of active sand dunes on
549 the Canadian prairies and relation to recent climate variations. *Geomorphology* 68,
550 131-147.

551 Jankowski, N. R., Jacobs, Z., 2018. Beta dose variability and its spatial
552 contextualisation in samples used for optical dating: An empirical approach to
553 examining beta microdosimetry. *Quaternary Geochronology* 44, 23-37.

554 Kar, A., 1987. Origin and transformation of longitudinal sand dunes in the Indian
555 desert. *Zeitschrift fur Geomorphologie* 31, 311-337.

556 Kar, A., 1993. Aeolian processes and bedforms in the Thar Desert. *Journal of Arid*
557 *Environments* 25, 83-96.

558 Kar, A., 2014. The Thar or the Great Indian Sand Desert. In *Landscapes and*
559 *Landforms of India* 79-90. Springer, Dordrecht.

560 Kar, A., Felix, C., Rajaguru, S. N., Singhvi, A. K., 1998. Late Holocene growth and
561 mobility of a transverse dune in the Thar Desert. *Journal of Arid Environments* 38, 175-
562 185.

563 Kar, A., Singhvi, A. K., Rajaguru, S. N., Juyal, N., Thomas, J. V., Banerjee, D., Dhir,
564 R. P., 2001. Reconstruction of the late Quaternary environment of the lower Luni
565 plains, Thar Desert, India. *Journal of Quaternary Science: Published for the*
566 *Quaternary Research Association* 16, 61-68.

567 Kreutzer, S., Dietze, M., Burow, C., Fuchs, M. C., Schmidt, C., Fischer, M., Friedrich,
568 J., 2017. Luminescence: Comprehensive luminescence dating data analysis. R
569 package version 0.7.3.

570 Kristensen, J. A., Thomsen, K. J., Murray, A. S., Buylaert, J. P., Jain, M., Breuning-
571 Madsen, H., 2015. Quantification of termite bioturbation in a savannah ecosystem:
572 application of OSL dating. *Quaternary Geochronology* 30, 334-341.

573 Kumar, M., Goossens, E., Goossens, R., 1993. Assessment of sand dune change
574 detection in Rajasthan Thar Desert, India. *International Journal of Remote*
575 *Sensing* 14, 1689-1703.

576 Lancaster, N., 1982. Linear dunes. *Progress in Physical Geography* 6, 475-504.

577 Lancaster, N., Wolfe, S., Thomas, D.S.G., Bristow, C., Bubenzer, O., Burrough, S. L.,
578 Duller, G., Halfen, A., Hesse, P.P., Roskin, J. and Singhvi, A. K., 2016. The INQUA
579 dunes atlas chronologic database. *Quaternary international* 410, 3-10.

580 Leighton, C. L., Bailey, R. M., Thomas, D. S. G., 2013. The utility of desert sand dunes
581 as Quaternary chronostratigraphic archives: evidence from the northeast Rub'al
582 Khali. *Quaternary Science Reviews* 78, 303-318.

583 Livingstone, I., Thomas, D. S. G., 1993. Modes of linear dune activity and their
584 palaeoenvironmental significance: an evaluation with reference to southern African
585 examples. *Geological Society, London, Special Publications* 72, 91-101.

586 Lomax, J., Hilgers, A., Wopfner, H., Grün, R., Twidale, C. R., Radtke, U., 2003. The
587 onset of dune formation in the Strzelecki Desert, South Australia. *Quaternary Science*
588 *Reviews* 22, 1067-1076.

589 Mayya, Y. S., Morthekai, P., Murari, M. K., Singhvi, A. K., 2006. Towards quantifying
590 beta microdosimetric effects in single-grain quartz dose distribution. *Radiation*
591 *Measurements* 41, 1032-1039.

592 Moharana, P. C., Gaur, M. C., Choudhary, C., Chauhan, J. S., Rajpurohit, R. S., 2013.
593 A system of geomorphological mapping for western Rajasthan with relevance for
594 agricultural land use. *Annals of Arid Zone* 52, 163-180.

595 Munyikwa, K., 2005. The role of dune morphogenetic history in the interpretation of
596 linear dune luminescence chronologies: a review of linear dune dynamics. *Progress*
597 *in Physical Geography* 29, 317-336.

598 Murray, A. S., Funder, S., 2003. Optically stimulated luminescence dating of a Danish
599 Eemian coastal marine deposit: a test of accuracy. *Quaternary Science Reviews* 22,
600 1177-1183.

601 Murray, A. S., Wintle, A. G., 2003. The single aliquot regenerative dose protocol:
602 potential for improvements in reliability. *Radiation measurements* 37, 377-381.

603 Murray, A.S., Wintle, A. G., Wallinga, J., 2002. Dose estimation using quartz OSL in
604 the non-linear region of the growth curve. *Radiation Protection Dosimetry* 101, 371-
605 374.

606 Nathan, R. P., Thomas, P. J., Jain, M., Murray, A. S., Rhodes, E. J., 2003.
607 Environmental dose rate heterogeneity of beta radiation and its implications for
608 luminescence dating: Monte Carlo modelling and experimental validation. *Radiation*
609 *Measurements* 37, 305-313.

610 O'Connor, P. W., Thomas, D. S. G., 1999. The timing and environmental significance
611 of late Quaternary linear dune development in western Zambia. *Quaternary*
612 *Research* 52, 44-55.

613 Olley, J. M., Pietsch, T., Roberts, R. G., 2004. Optical dating of Holocene sediments
614 from a variety of geomorphic settings using single grains of
615 quartz. *Geomorphology* 60, 337-358.

616 Pandey, S., Singh, S., Ghose, B., 1964. Orientation, distribution and origin of sand
617 dunes in the central Luni basin. In *Proceedings, Symposium on Problems of Indian*
618 *Arid Zone*, 84-91.

619 Parton, A., Farrant, A. R., Leng, M. J., Telfer, M. W., Groucutt, H. S., Petraglia, M. D.,
620 Parker, A. G., 2015. Alluvial fan records from southeast Arabia reveal multiple
621 windows for human dispersal. *Geology* 43, 295-298.

622 Prescott, J. R., Hutton, J. T., 1994. Cosmic ray contributions to dose rates for
623 luminescence and ESR dating: large depths and long-term time variations. *Radiation*
624 *measurements* 23, 497-500.

625 Roskin, J., Porat, N., Tsoar, H., Blumberg, D. G., Zander, A. M., 2011a. Age, origin
626 and climatic controls on vegetated linear dunes in the northwestern Negev Desert
627 Israel. *Quaternary Science Reviews* 30, 1649-1674.

628 Roskin, J., Tsoar, H., Porat, N., Blumberg, D. G., 2011b. Palaeoclimate interpretations
629 of Late Pleistocene vegetated linear dune mobilization episodes: evidence from the
630 northwestern Negev dunefield, Israel. *Quaternary Science Reviews* 30, 3364-3380.

631 Saxena, S. K., Singh, S., 1976. Some observations on the sand dunes and vegetation
632 of Bikaner district in Western Rajasthan, India. *Annals of Arid Zone*.

633 Singhvi, A. K., Kar, A., 2004. The aeolian sedimentation record of the Thar
634 Desert. *Journal of Earth System Science* 113, 371-401.

635 Singhvi, A. K., Porat, N., 2008. Impact of luminescence dating on geomorphological
636 and palaeoclimate research in drylands. *Boreas* 37, 536-558.

637 Singhvi, A. K., Williams, M. A. J., Rajaguru, S. N., Misra, V. N., Chawla, S., Stokes,
638 Chauhan, N., Francis, T., Ganjoo, R., Humphreys, G. S., 2010. A ~200 ka record of
639 climatic change and dune activity in the Thar Desert, India. *Quaternary Science*
640 *Reviews* 29, 3095-3105.

641 Srivastava, A., Thomas, D. S. G., Durcan, J. A., 2019. Holocene dune activity in the
642 Thar Desert, India. *Earth Surface Processes and Landforms* 44, 1407-1418.

643 Stokes, S., Thomas, D. S. G., Shaw, P. A., 1997. New chronological evidence for the
644 nature and timing of linear dune development in the southwest Kalahari
645 Desert. *Geomorphology* 20, 81-93.

646 Stone, A. E. C., Thomas, D. S. G., 2008. Linear dune accumulation chronologies from
647 the southwest Kalahari, Namibia: challenges of reconstructing late Quaternary
648 palaeoenvironments from aeolian landforms. *Quaternary Science Reviews* 27, 1667-
649 1681.

650 Telfer, M. W., Bailey, R. M., Burrough, S. L., Stone, A. E. S., Thomas, D. S. G., Wiggs,
651 G. F. S., 2010. Understanding linear dune chronologies: insights from a simple
652 accumulation model. *Geomorphology* 120, 195-208.

653 Telfer, M. W., Hesse, P. P., 2013. Palaeoenvironmental reconstructions from linear
654 dunefields: recent progress, current challenges and future directions. *Quaternary
655 Science Reviews* 78, 1-21.

656 Telfer, M. W., Thomas, D. S. G., 2007. Late Quaternary linear dune accumulation and
657 chronostratigraphy of the southwestern Kalahari: implications for aeolian
658 palaeoclimatic reconstructions and predictions of future dynamics. *Quaternary
659 Science Reviews* 26, 2617-2630.

660 Thomas, D. S. G., 1992. Desert dune activity: concepts and significance. *Journal of
661 Arid Environments* 22, 31-38.

662 Thomas, D. S. G., 2013. Reconstructing paleoenvironments and palaeoclimates in
663 drylands: what can landform analysis contribute? *Earth Surface Processes and
664 Landforms* 38, 3-16.

665 Thomas, D. S. G., Shaw, P. A., 1991. *The Kalahari Environment*. Cambridge
666 University Press.

667 Thomas, J. V., Kar, A., Kailath, A. J., Juyal, N., Rajaguru, S. N., Singhvi, A. K., 1999.
668 Late Pleistocene-Holocene-history of aeolian accumulation in the Thar Desert, India.
669 *Zeitschrift fur Geomorphologie Supplementband* 181-194.

670 Thomsen, K. J., Murray, A. S., Bøtter-Jensen, L., 2005. Sources of variability in OSL
671 dose measurements using single grains of quartz. *Radiation Measurements* 39, 47-
672 61.

673 Thomsen, K. J., Murray, A. S., Jain, M., 2012. The dose dependency of the over-
674 dispersion of quartz OSL single grain dose distributions. *Radiation Measurements* 47,
675 732-739.

676 Tsoar, H., 1989. Linear dunes-forms and formation. *Progress in Physical
677 Geography* 13, 507-528.

678 Tsoar, H., Blumberg, D. G., Wenkart, R., 2008. Formation and geomorphology of the
679 North-Western Negev sand dunes. In *Arid dune ecosystems*, 25-48. Springer, Berlin,
680 Heidelberg.

681 Tsoar, H., Møller, J. T., 1986. The role of vegetation in the formation of linear sand
682 dunes. *Aeolian geomorphology* 75-95.

683 Verstappen, H. T., 1968. On the origin of longitudinal seif dunes. Zeitschrift für
684 Geomorphologie NF 12, 200-220.

685 Wasson, R. J., Rajaguru, S. N., Misra, V. N., Agrawal, D. P., Dhir, R. P., Singhvi, A.
686 K., Rao, K. K., 1983. Geomorphology, late Quaternary stratigraphy and
687 palaeoclimatology of the Thar dunefield.

688 Wintle, A. G., Murray, A. S., 2006. A review of quartz optically stimulated
689 luminescence characteristics and their relevance in single-aliquot regeneration dating
690 protocols. Radiation measurements 41, 369-391.

691

692